

B -flavour anomalies in $b \rightarrow sll$ and $b \rightarrow cl\nu_\ell$ transitions at LHCb

Alessandra Gioventù^{*†}

Instituto Galego de Física de Altas Enerxías (IGFAE), Universidade de Santiago de Compostela

E-mail: alessandra.gioventu@cern.ch

In the Standard Model (SM) of particle physics, the muon and the tau particles are simply heavier copies of the electron, coupling with gauge bosons independently of their generation. This property is called Lepton Flavour Universality (LFU). In models beyond the SM, LFU can be naturally violated with new physics particles that couple differently with respect to the lepton generations. Over the last few years, several hints of LFU violation have been reported in both $b \rightarrow c$ and $b \rightarrow s$ transitions. An overview of the measurements performed by LHCb during Run 1 ($\sqrt{s} = 7 - 8$ TeV) and part of Run 2 ($\sqrt{s} = 13$ TeV) is reported.

XXVII International Workshop on Deep-Inelastic Scattering and Related Subjects - DIS2019

8-12 April, 2019

Torino, Italy

^{*}Speaker.

[†]On behalf of the LHCb Collaboration

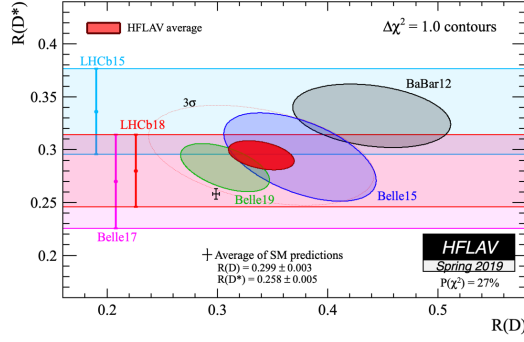


Figure 1: Combined measurements of the ratios $R(D)$ and $R(D^*)$ performed by B -factories (BaBar and Belle) and LHCb, as of Spring 2019 [3]. The SM prediction is in black, the combined measurements are represented as ellipses while the $R(D^*)$ alone are vertical lines.

1. Introduction

The Standard Model (SM) of particle physics organises leptons and quarks in three families or generations, distinguished only by their masses. The SM assumes that the couplings between leptons and the electroweak gauge bosons (Z^0, W^\pm) are independent of the generation. This property is known as Lepton Flavour Universality (LFU). Many new physics (NP) scenarios predict LFU-violating processes.

The LHCb experiment [1] is dedicated to heavy flavour physics measurements and it is the best suited environment to search for indirect evidence of NP. In order to exploit the fact that b quark pairs are produced in the same forward or backward hemisphere with a small angle with respect to the beam direction, the LHCb detector has the structure of a forward spectrometer, covering the pseudorapidity range $2.0 < \eta < 5.0$. The main features of the detector are the excellent vertex and impact parameter resolutions ($\sigma_{IP} \sim 20 \mu\text{m}$ [2]). They provide the distinction between the proton interaction vertex and the b hadron decay vertex with high precision.

The LHCb data is divided in two sets. The Run 1 data sample includes proton collisions at centre-of-mass energies of 7 and 8 TeV, recorded from 2010 to 2012, while during Run 2 (2015-2018) pp collisions occurred at $\sqrt{s} = 13$ TeV. The LHCb detector has performed very well in these years of data-taking, collecting a total of 3.0 fb^{-1} of data in Run 1 and 5.7 fb^{-1} in Run 2 [2]. The majority of the measurements presented here are based on the LHCb Run 1 data sample, only the $R(K)$ result includes part of the Run 2 data sample.

The recent experimental results on semileptonic decays, performed by the B -factories (Belle, BaBar) and LHCb, have shown tension with respect to the SM predictions. These measurements have been obtained from the study of semileptonic $b \rightarrow c\ell\nu_\ell$ decays where $\ell = \tau, \mu$. In the SM they are tree-level processes, mediated by a W boson with a branching fraction of the order of a few percent and they are sensitive to NP. The other set of measurements involves $b \rightarrow s\ell^+\ell^-$ transitions, where ℓ stands for an electron or a muon. In the SM these are Flavour Changing Neutral Currents (FCNC) processes, occurring only at loop level: through a box diagram with two W bosons, or a penguin diagram with the exchange of a γ or a Z boson. Hence, this kind of transitions is sensitive to NP at the tree or at the loop level.

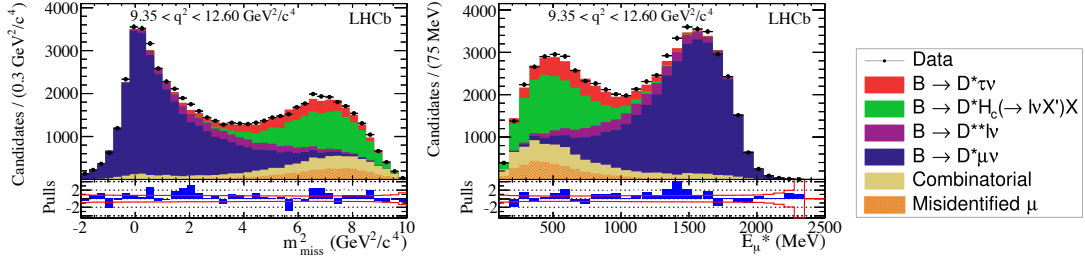


Figure 2: Fit results for the measurement of $R(D^*)$, with muonic final state. Distribution of m_{miss}^2 (left) and E_{μ}^* (right) in the highest bin of q^2 ($[9.35, 12.60] \text{ GeV}^2/c^4$) [4]. Data points are in black and the different colours represent the different fit components, shown in the legend on the right.

2. Measurements in semitauonic $b \rightarrow c\ell\nu_{\ell}$ transitions

In order to test LFU, one interesting observable is the ratio $R(H_c)$, defined as

$$R(H_c) = \frac{BR(H_b \rightarrow H_c \tau^- \bar{\nu}_{\tau})}{BR(H_b \rightarrow H_c \mu^- \bar{\nu}_{\mu})}, \quad \text{where } H_c = D^*, D^+, J/\psi, \dots \quad \text{and } H_b = B^{\pm}, B^0, B_c. \quad (2.1)$$

This partly cancels experimental and theoretical uncertainties, since the hadronic resonant state is identical. In the SM $R(H_c)$ deviates from unity, due to the different lepton masses. The measurements of $R(D)$ and $R(D^*)$ show some tensions from the expected values. In particular, the significance of these tensions with respect to the SM predictions for $R(D)$ and $R(D^*)$ is ~ 1.4 and ~ 2.5 standard deviations (σ), respectively [3]. The combined $R(D)$ and $R(D^*)$ measurements show an overall tension with the SM prediction of about 3.08σ , as shown in Fig. 1. These processes have two main experimental features. First of all, due to the design of the LHCb detector, it is not possible to reconstruct the neutrino momentum using the missing transverse energy or kinematical constraints. Secondly, it is possible to reconstruct the tau using two different decay channels: the muonic decay $\tau^- \rightarrow \mu^- \bar{\nu}_{\mu} \nu_{\tau}$ and the hadronic one $\tau^- \rightarrow \pi^- \pi^+ \pi^- \nu_{\tau}$.

2.1 $R(D^*)$ muonic

The first measurement of $R(D^*)$ by LHCb was performed using the $\bar{B}^0 \rightarrow D^{*+} \ell^- \bar{\nu}_{\ell}$ decay. The tau is reconstructed exploiting the muonic final state and the D^* is reconstructed through the $D^{*-} \rightarrow \bar{D}^0 (\rightarrow K^+ \pi^-) \pi^-$ decay [4]. In order to take into account the missing neutrino a kinematical approximation is used. Since the boost of the \bar{B}^0 along the z axis is higher than the one of its decay products in the \bar{B}^0 rest frame, its momentum is approximated as $(p_z)_B = \frac{m_B}{m_{D^* \mu}} (p_z)_{(D^* \mu)}$.

A 3D binned template fit is performed to separate the tau and the muon channels. This includes the 4-momentum transfer $q^2 = (p_B - p_{D^*})^2$, the missing mass $m_{\text{miss}}^2 = (p_B - p_{D^*} - p_{\mu})^2$ and the energy of the muon in the \bar{B}^0 rest frame, E_{μ}^* . As represented in Fig. 2.1, the sample is dominated by the normalisation channel and the main contribution to the background is due to the $\bar{B}^0 \rightarrow D^{*+} \ell^- \bar{\nu}_{\ell} X$ decay. The final result is $R(D^*) = 0.366 \pm 0.027$ (stat) ± 0.030 (syst), where the two uncertainty components are the statistical and the systematic one, respectively.

2.2 $R(J/\psi)$ muonic

An expansion in the B_c sector of this measurement can be done exploiting the $B_c^+ \rightarrow J/\psi \ell^+ \nu_{\ell}$ decay, where $\tau^+ \rightarrow \mu^+ \nu_{\mu} \bar{\nu}_{\tau}$ [5]. The J/ψ meson is reconstructed using the $\mu^+ \mu^-$ final state,

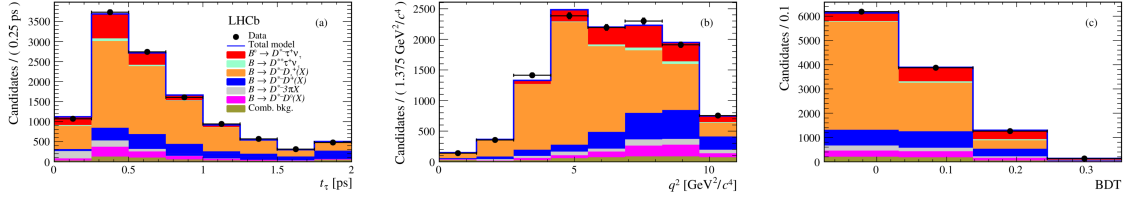


Figure 3: Projections of the fit of the hadronic $R(D^*)$ measurement. From left to right, distributions of the τ decay time t_τ , the 4-momentum transfer q^2 and the BDT output [6]. The different components are represented with different colours.

and the B_c^+ momentum is approximated in the same way as in the $R(D^*)$ measurement. The ratio $R(J/\psi)$ is obtained from a three-dimensional binned fit to m_{miss}^2 , the B_c^+ decay time and $Z[q^2, E_\mu^*]$, a discrete variable representing eight bins in (E_μ^*, q^2) .

The final result is $R(D^*) = 0.71 \pm 0.17$ (stat) ± 0.18 (syst), deviating from the SM of $\sim 2\sigma$. The uncertainties are originated in the size of the B_c^+ sample and the poor knowledge of the form factors involved in the transition.

2.3 $R(D^*)$ hadronic

The first measurement of $R(D^*)$ with the 3-prong final state of the tau decay has been published by LHCb in 2017 [6]. The same visible final state for the normalisation and the signal channels $\tau^+ \rightarrow \pi^+ \pi^- \pi^+ (\pi^0) \bar{\nu}_\tau$ is used in order to reduce systematic effects, measuring the quantity $K(D^{*-})$, defined as

$$K(D^{*-}) = \frac{BR(B^0 \rightarrow D^{*-} \tau^+ \nu_\tau)}{BR(B^0 \rightarrow D^{*-} \pi^+ \pi^- \pi^+)}. \quad (2.2)$$

In this way, $R(D^*)$ is then obtained using the averages from external measurements of $BR(B^0 \rightarrow D^{*-} \pi^+ \pi^- \pi^+)$ and $BR(B^0 \rightarrow D^{*-} \mu^+ \nu_\mu)$ [7, 8, 9].

Considering the hadronic decay of the tau allows to exploit its decay vertex as a tool to discriminate against background events. As a consequence, one of the main contributions to the $B^0 \rightarrow D^{*-} \pi^+ \pi^- \pi^+ (X)$ background is decreased by requiring a displacement between the D^* and the τ decay vertices ($\Delta z > 4\sigma_{\Delta z}$).

The second main background source is due to doubly charmed $B \rightarrow D^{*-} D_s^+ (X)$ decays, where B stands for B^+, B^0, B_s^0 . It is rejected using a multivariate analysis method (Boosted Decision Tree, BDT), which exploits the differences in the dynamics of the final state generated by the decay of the D_s^+ with respect to the one from the τ decay.

The yield of the normalisation channel is obtained from an unbinned fit to the invariant mass of the $D^{*-} \pi^+ \pi^- \pi^+$ system. A 3-dimensional fit to data is performed to extract the yields, where the variables are q^2 , the τ decay time t_τ and the output of the BDT, as shown in Fig. 3.2. The measured value of $R(D^*)$ is 0.291 ± 0.019 (stat) ± 0.026 (syst) ± 0.013 (ext), where the last contribution to the uncertainty is due to the values taken from the external inputs of the branching ratios.

3. Measurements in $b \rightarrow s\ell\ell$ transitions

In $b \rightarrow s\ell^+\ell^-$ processes the quantity $R(H_s)$ is studied. It is defined in Eq. 3.1 within a given

range of q^2 . The SM predicts its value equal to one with a precision of the order of 1% [10, 11].

$$R(H_s) = \frac{BR(H_b \rightarrow H_s \mu^+ \mu^-)}{BR(H_b \rightarrow H_s e^+ e^-)} \quad \text{where } H_s = K^{*0}, K^+, \dots \quad \text{and } H_b = B^+, B^0 \quad (3.1)$$

The main challenge of these measurements is the presence of the electrons in the final state. In order to reduce systematic uncertainties induced by the different reconstruction of the final states, the double ratio $R(H_s)$ is considered, *i.e.*

$$R(H_s) = \frac{BR(H_b \rightarrow H_s \mu^+ \mu^-)}{BR(H_b \rightarrow H_s J/\psi(\rightarrow \mu^+ \mu^-))} \bigg/ \frac{BR(H_b \rightarrow H_s e^+ e^-)}{BR(H_b \rightarrow H_s J/\psi(\rightarrow e^+ e^-))}. \quad (3.2)$$

It takes advantage of the fact that the topologies of $J/\psi \rightarrow \ell^+ \ell^-$ and the non-resonant channels are similar. Moreover, since the effects of the bremsstrahlung emission depend on where the radiation occurs with respect to the dipole magnet, a recovery procedure is performed to improve energy resolution.

Finally, the yields are extracted from a simultaneous fit to the B mass distribution $M(H_s \ell^+ \ell^-)$ to the resonant and non-resonant channels.

3.1 $R(K^*)$

LHCb measured $R(K^*)$ in the lower and central bin of q^2 , [0.045, 1.1] and [1.1, 6.0] GeV^2/c^4 respectively [12]. The K^{*0} is reconstructed from $K^{*0} \rightarrow K^+ \pi^-$. The LHCb result is the most precise up to date. For the lower and central bins $R(K^*) = 0.66^{+0.11}_{-0.07}$ (stat) ± 0.03 (syst) and $R(K^*) = 0.69^{+0.11}_{-0.07}$ (stat) ± 0.05 (syst) respectively, where the first uncertainty is due to statistics and the second one to systematic effects. The deviation from the SM predictions for the lower and the central bin is at the level of $\sim 2.2\sigma$ and $\sim 2.4\sigma$, respectively.

3.2 $R(K)$

$R(K)$ is measured studying the decay $B^+ \rightarrow K^+ \ell^+ \ell^-$ in the $1.1 < q^2 < 6.0 \text{ GeV}^2/c^4$ [13]. The latest result has been obtained analysing the Run 1 and 2015+2016 data samples, corresponding to an integrated luminosity of 5.0 fb^{-1} . The fit results to the $M(K \ell^+ \ell^-)$ distribution are shown in Fig. 4. The main contributions to the background are due to the combinatorial background, which is higher in the electron final state $K^+ e^+ e^-$. The final result is $R(K) = 0.846^{+0.060}_{-0.054}$ (stat) $^{+0.016}_{-0.014}$ (syst). It deviates from the SM in about 2.5σ .

4. Conclusions

Testing LFU is a potential road to look for NP. The experimental results of LFU tests on semileptonic and rare decays show discrepancies with respect to the SM, including the most recent $R(K)$ measurement.

LHCb has performed very well in both Run 1 and Run 2, collecting a data sample of an integrated luminosity of 9.2 fb^{-1} . At present, LHCb measurements of $b \rightarrow c \ell \nu_\ell$ ($R(D^*)$ and $R(J/\psi)$) and $b \rightarrow s \ell^+ \ell^-$ ($R(K^*)$ and $R(K)$) transitions are the most precise.

Uncertainties are expected to improve [14] and in the near future more measurements including the whole data sample will be presented. Moreover, also external uncertainties are expected to improve, thanks to the prospected measurements of Belle II, BESIII and CMS.

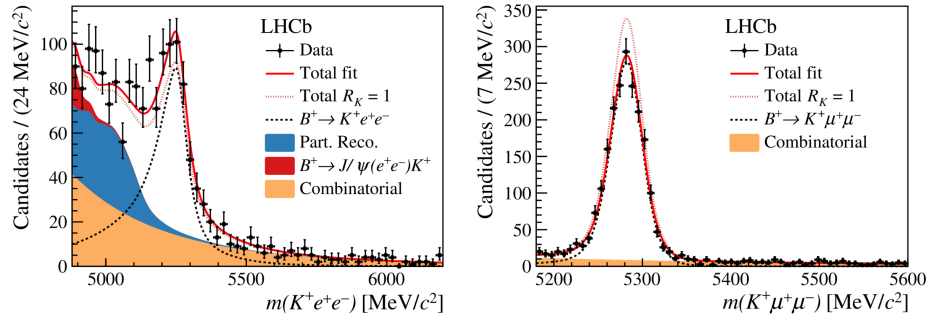


Figure 4: $M(K\ell^+\ell^-)$ distributions after the fit for the e (left) and μ (right) final states [13]. The different colours represent the different sources of background.

References

- [1] LHCb collaboration, *The LHCb detector at the LHC*, *JINST* **3** (2008) S08005.
- [2] LHCb COLLABORATION collaboration, *LHCb detector performance*, *Int. J. Mod. Phys. A* **30** (2015) 1530022 [1412.6352].
- [3] HEAVY FLAVOR AVERAGING GROUP collaboration, *Averages of b-hadron, c-hadron, and τ -lepton properties as of summer 2016*, *Eur. Phys. J. C* **77** (2017) 895 [1612.07233].
- [4] LHCb collaboration, *Measurement of the ratio of branching fractions $\mathcal{B}(\bar{B}^0 \rightarrow D^{*+}\tau^- \bar{\nu}_\tau)/\mathcal{B}(\bar{B}^0 \rightarrow D^{*+}\mu^- \bar{\nu}_\mu)$* , *Phys. Rev. Lett.* **115** (2015) 111803 [1506.08614].
- [5] LHCb collaboration, *Measurement of the ratio of branching fractions $\mathcal{B}(B_c^+ \rightarrow J/\psi\tau^+ \nu_\tau)/\mathcal{B}(B_c^+ \rightarrow J/\psi\mu^+ \nu_\mu)$* , *Phys. Rev. Lett.* **120** (2018) 121801 [1711.05623].
- [6] LHCb collaboration, *Test of lepton flavor universality by the measurement of the $B^0 \rightarrow D^{*-}\tau^+ \nu_\tau$ branching fraction using three-prong τ decays*, *Phys. Rev. D* **97** (2018) 072013 [1711.02505].
- [7] LHCb collaboration, *Study of $B^0 \rightarrow D^{*-}\pi^+\pi^-\pi^+$ and $B^0 \rightarrow D^{*-}K^+\pi^-\pi^+$ decays*, *Phys. Rev. D* **87** (2013) 092001 [1303.6861].
- [8] BABAR collaboration, *Measurement of the $B^0 \rightarrow D^{*-}\pi^+\pi^-\pi^+$ branching fraction*, *Phys. Rev. D* **94** (2016) 091101 [1609.06802].
- [9] BELLE collaboration, *Observation of $B^0 \rightarrow D^{*-}(5\pi)^+$, $B^+ \rightarrow D^{*-}(4\pi)^{++}$ and $B^+ \rightarrow \bar{D}^{*0}(5\pi)^+$* , *Phys. Rev. D* **70** (2004) 111103 [hep-ex/0409008].
- [10] C. Bobeth, G. Hiller and G. Piranishvili, *Angular distributions of $B \rightarrow K\ell\ell$ decays*, *Journal of High Energy Physics* **2007** (2007) 040.
- [11] M. Bordone, G. Isidori and A. Pattori, *On the standard model predictions for R_K and R_{K^*}* , *The European Physical Journal C* **76** (2016) 440.
- [12] LHCb collaboration, *Test of lepton universality with $B^0 \rightarrow K^{*0}\ell^+\ell^-$ decays*, *JHEP* **08** (2017) 055 [1705.05802].
- [13] LHCb collaboration, *Search for lepton-universality violation in $B^+ \rightarrow K^+\ell^+\ell^-$ decays*, *Phys. Rev. Lett.* **122** (2019) 191801 [1903.09252].
- [14] S. Bifani, S. Descotes-Genon, A. R. Vidal and M.-H. Schune, *Review of lepton universality tests in b decays*, *Journal of Physics G: Nuclear and Particle Physics* **46** (2018) 023001.